www.gondwanags.org.in
Research Article

ISSN : 2455-1953
JGSR
Journal of Geosciences Research
Vol. 9, No.2, July, 2024, pp. 108-115

Morphotectonic Study of Iring watershed, Tamenglong District, Manipur, India

Yumkhaibam Sanjitkumar Singh[1]*, Yumkhaibam Rajesh Singh[1]
Manichandra Sanoujam[2] and Arun Kumar[1]

[1]*Department of Earth Sciences, Manipur University, Imphal-795003(MN), India*
[2]*Seismological Observatory, Manipur University, Imphal-795003(MN), India*
*(*Corresponding Author, E-mail: ysksingh@gmail.com)*

Abstract

The primary focus of study is on the morphotectonic investigation of the Iring watershed in the Manipur district of Tamenglong. Various morphotectonic factors were studied using data from Aster-DEM, SENTINEL-2 satellite, Survey of India Topographical Maps, and field verification. Drainage Basin Asymmetry (AF), Transverse Topographic Symmetry (T), Basin Elongation Ratio (Eb), and Valley Floor Width to Valley Height ratio (V_f) are a few examples of geomorphic indices that were examined. It was found that the 118.67 km^2 basin is tectonically active, as evidenced by structural characteristics and geomorphic parameter values. River stress knick sites are indicated by regions with an SLK index greater than 10. The watershed exhibits asymmetry, as indicated by the average T value of 0.195. Actively incising V-shaped valleys linked to uplift are indicated by V_f values between 0.192 and 0.263. The river is migrating to the western side due to elevation on the eastern side, as shown by the AF result of 47.72%. A basin that is extended and experiencing tectonic activity has a basin elongation ratio of 0.66. The hypsometric curve and hypsometric integral (~50%) indicate that the erosion process in the basin is at its early mature stage.

Keywords: Morphotectonic Indices, Active Tectonics, Geology, Morphometry, Drainage Basin, Hypsometry

Introduction

In order to examine the landforms and relative level of tectonic activity of the Iring watershed, a number of geomorphic indices are estimated. Aster-DEM, satellite data, and topographic maps are used to compute various quantified geomorphic indices, which provide important details about the tectonic history of a region (Keller, 1986). Utilising geomorphological, structural, and neotectonism data in a constructive multidisciplinary manner provides valuable insights into the active tectonics of a region (Wells *et al*., 1988). We therefore analysed six geomorphic indices: stream gradient index (Hack, 1973), hypsometric integral (HI), (Strahler, 1952) along with convex-up hypsometric curve, drainage basin asymmetry factor (AF), (Hare and Gardner, 1985; Keller and Pinter, 2002), basin elongation ratio (Eb), (Schumm, 1956), ratio of valley floor width to valley height (Vf), (Bull and McFadden, 1977), and transverse topography symmetry factor (T). These features are very useful and important indicators in exploring the relative tectonic activity (Bull and McFadden 1977; Keller and Pinter 1996; Burbank and Anderson, 2001). The aforementioned indicators are used to assess the basin's relative tectonic activity level and to corroborate the findings of the SL-index study conducted in the western portion of the Imphal valley. Further, all of the calculated geomorphic indices are connected in order to comprehend the relative tectonic activities and tectonic history of the research area. Numerous tectonically active areas have proven the value of this type of methodology, including the northeastern Indian Shillong Plateau (Mukteshwar, 2019), Costa Rica's Pacific Coast (Wells *et al*., 1988), the Southwest United States (Rockwell *et al*., 1985), Spain's Mediterranean Coast (Cox, 1994), the southwest Sierra Nevada of Spain (El Hamdouni *et al*., 2007), and Kashmir Valley (Ahmad and Bhat 2012; Ahmad *et al*., 2013). Additionally, we assessed and linked the morphometric studies' findings with field-based geomorphological data.

(Received : 06 December 2023 ; Revised Form Accepted : 20 April 2024)
https://doi.org/10.56153/g19088-023-0192-58

Location of Study Area and Its Drainage Characteristics

The Iring watershed lies on the western side of the Imphal valley, between latitudes 25°00'38.19" and 24° 51' 24.47" N and longitudes 93°43'57.56" and 93° 35' 37.52" E. The research location is located in the Indian state of Manipur's Tamenglong district (Fig. 1). It has a total catchment area of 118.67 Km^2. The Ijai River flows on its eastern side, while the Tupul River flows on its southern side, where the rivers confluence at Noney.

The drainage characteristics of the Iring River Basin are shown in Fig. 2. It originates from Taduining of Tamenglong District and extended up to Noney of Noney District, Manipur where it confluences with Ijai River. It generally flows in the direction NE to SW up to Noney of Noney District with a perennial

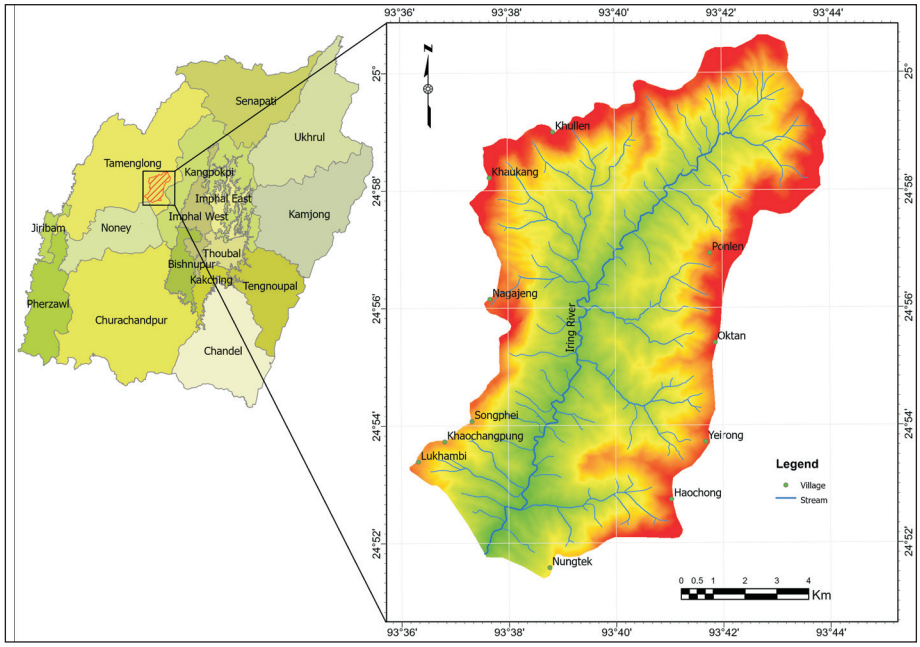

Fig.1. Location map of the study area

course of about 23.89 km. The Iring river basin generally shows dendritic to trellis drainage pattern in general.

Regional Geology and Tectonic Setup

The principal geological formations in Manipur are Tertiary and Cretaceous sediments, with some igneous and metamorphic rocks, as the region is part of the Indo-Mayanmar Ranges (IMR), an arcuate-shaped tectonic belt. Four groups *viz.* Disang, Barail, Surma, and Tipam make up sedimentary sequence of Manipur. The majority of sediments of the Tertiary age are sandstones, shales, siltstones, and mudstones, with smaller amounts of oceano-pelagic sediments like limestone and chert of Cretaceous age. However, Disang and Barial Group of rocks cover the study area (Fig.3). Mallet (1876) used the term "Disang" to describe a coarse, splintery shale that ranges in colour from dark grey to black and is interbedded with siltstone and fine-grained sandstone. The Disang formation is divided into Upper Disang and Lower Disang. Upper Disang is characterized by siltstone and fine sandstone layers alternating with dark grey, splintery shales. Meanwhile, Lower Disang consists of dark grey shales interspersed with mudstone and sandstone, displaying a laminated and arenaceous nature. Evans (1932) first used the word "Barail" to refer to a massive, thick column of shales and arenaceous layers that lay above the Disang and Jaintia Groups. Three formations have been further separated out of this group: the Liaisong Formation, Jenam Formation, and Renji Formation. Within the lowest level is the Laisong Formation, which is distinguished by shale alteration and fine- to medium-grained sandstones exhibiting a characteristic turbidite pattern. The Jenam Formation, which lies directly above it, is characterised by large areas of carbonaceous shale interspersed with silt and sandstone bands. Sandstones that are large to bedded define the uppermost formation, the Renji Formation.

The Disang Group along the anticlinal axis of the Langka Fault dominates the primary central portion of the research region. The Barail formation, which ranges in age from Oligocene to Upper Eocene and is the primary flysch deposit of the area, dominates the western and eastern portions of the Disang formation in the study area (Table 1). The structural and tectonic environment of the study area is primarily one of transition between the Naga-Patkoi Hills' NE-SW trend and the Chin Hills' N-S trend in Mizoram. It is bounded by Kangchup synclinal axis in the East and by Nungba

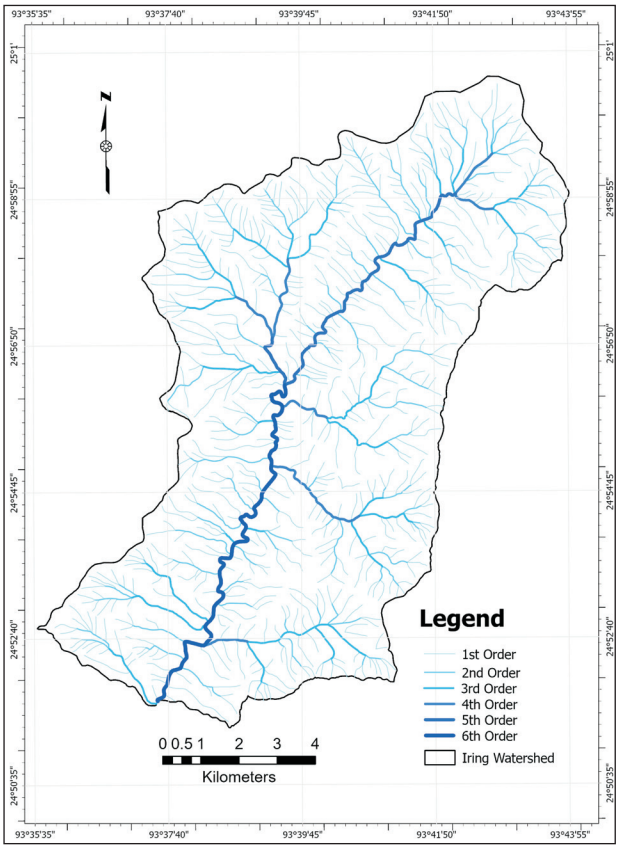

Fig. 2. Drainage characteristics of Iring watershed.

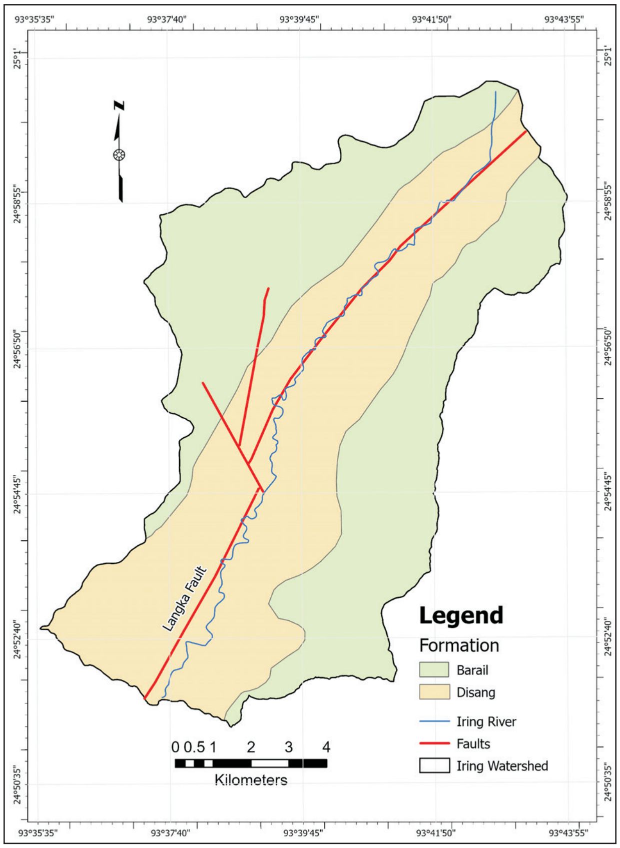

Fig. 3. Geological map of the study area (GSI, 1992).

Thrust in the west. The rock formation of the area generally follows a NNE-SSW lithological and tectonic trend, with occasional variations to N-S, NE-SW, and NNW-SSE trends. The lithounits dip at varying angles towards the east or west, ranging from moderate to steep.

Material and Methods

In order to create a methodical plan for carrying out the work, Survey of India toposheets with numbers 83H/9 and 83G/12 on a 1:50,000 scale were utilised. Geomorphic indices such as the stream gradient index (SL index), valley floor width to valley height ratio (Vf), the drainage basin asymmetry factor (AF), the traverse topography asymmetry (T), the basin elongation ratio (Eb), the hypsometric curve, and the hypsometric integral were calculated using SENTINEL-2 satellite data, DEM, and Global Mapper V20.1 software, as these aid in the identification of tectonically active regions and specific sites in the study area (Keller 1986).

Geomorphic Indices and Results

Stream Gradient Index (SL)

According to Hack (1973), the stream gradient index provides information on the tectonic history and diastrophic forces that shaped the region. Additionally, the change in respect to slope, lithology, or added load is reflected in the Stream Gradient Index. (Hack, 1973; Keller and Pinter 1996; Burbank and Anderson, 2001; Azor *et al*., 2002; Chen *et al*., 2003; Perez-Pena *et al*., 2009, 2010; Tsodoulos *et al*., 2008) As a result, this offers a platform for assessing stream response to uplift and displacement associated with active tectonics.

Rivers typically form longitudinal profiles that are smooth and concave. However, lithology differences or tectonic activity cause these smooth concave longitudinal profiles to fluctuate. At sudden reaches, rivers that have experienced tectonic disturbance are expected to approach a convex type gradient profile (Snow and Slingerland 1987). Unusual high SL values in low- to uniform-resistant rocks may be a sign of active tectonics (Keller 1986). Thus, it is possible to interpret variations in river profiles as a reaction to continuing tectonism. For a specific reach of interest, the stream gradient index (SL) is defined as follows (Fig. 4; Hack 1973):

$$SL = \frac{\Delta H}{\Delta L} L$$

Where SL is the stream length gradient index, $\Delta H / \Delta L$ is the channel slope or gradient of the reach, and L is the total channel length from the point of interest where the index is being calculated upstream to the highest point on the channel.

The stream channel is also regarded by Hack (1973) as a continuous sequence of segments that vary in length and are all logarithmic in nature. The SL is normalised using the parameter K, which indicated how steep the logarithmic profile was for that particular segment. The Iring River's computed SL/K values rise up to 54.75 (Fig. 5).

Valley Floor Width to Valley Height Ratio

Valley floor width to valley height ratio (Vf) being a sensitive indicator that quantifies the valley incision in an uplifted area (Bull and McFadden, 1977). It can be defined as,

Table 1: Stratigraphic succession of the study area (Soibam, 1998)

Litho-Unit and Age	Description of rocks	
Alluvium (Quaternary to Holocene)	Brownish to dark grey sand, silt, clay deposits with considerable amount of cobbles and gravels.	
~~ Stratigraphic break ~~~~~		
Barail Group (Upper Eocene to Oligocene)	Jenam Formation	Intercalation of thinly bedded fine grained sandstone and shale
	~~ Gradational contact ~~~~~	
	Laisong Formation	Regressive sequence of shale, sandy shale and fine to medium grained sandstone with sedimentary structures like cross lamination, ripple marks etc.
	~~ Gradational contact ~~~~~	
Disang Group	Upper Disang	Dark grey splintery shales intercalated with siltstone and fine sandstone. Shales are arenaceous and laminated
	Lower Disang	Dark grey shales intercalated with mudstone and sandstone.

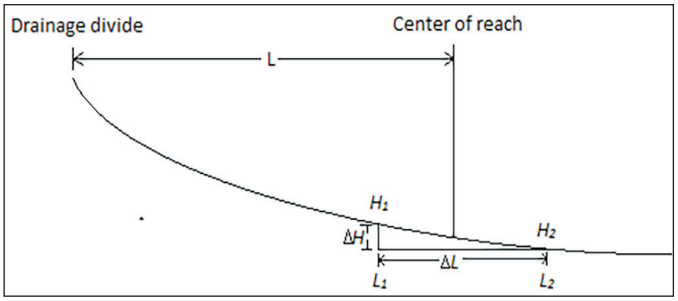

Fig. 4. Idealized diagram showing how SL index is calculated for a particular reach (after Hack, 1973).

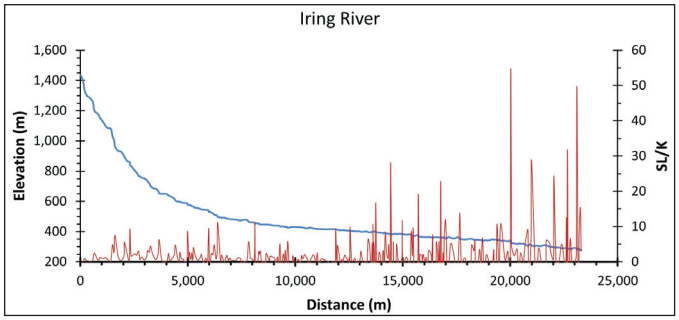

Fig. 5. Longitudinal profile along with SL/K of Iring river.

$$V_f = \frac{2V_{fw}}{(E_{ld} - E_{sc}) + (E_{rd} - E_{sc})}$$

Where, V_f is the valley floor width to valley height ratio, V_{fw} is the valley floor width of the valley for given profile at fixed length, E_{rd} and E_{ld} are the elevation of right and left divided for a given section line, respectively, facing downstream, and E_{sc} is the valley floor elevation (Fig. 6).

Actively incising streams are typically linked to upliftment and are represented as V-shaped valleys with V_f<1.0; moderately active tectonics are represented by V_f between 1.0 and 1.5, and major lateral erosion is experienced by U-shaped valleys with V_f >1.5 (Bull and McFadden, 1977).

The V_f values for the Iring river basin have been calculated for three sections *viz.*, AA', BB' and CC' (Fig.7a) and provided in the form of their profiles (Fig. 7b). The calculated values range from 0.192 to 0.263 (Table 2), suggesting V-shaped valley with streams actively incising associated with upliftment, indicating tectonically active study area.

Basin Elongation Ratio (Eb)

A quantitative morphometric measure that addresses a river basin's form is the basin elongation ratio (Bhattacharya *et al*., 2013), defined as the ratio of diameter of a circle having the same area as the basin to the maximum length of the basin (Schumm, 1956; Bull and McFadden, 1977). Because of ongoing thrusting and faulting in active locations, river basins experiencing active tectonism have an elongated shape (Burbank and Anderson, 2001; Sreedevi *et al*., 2004; Argyriou and Teeuw, 2016). According to Bull and McFadden (1977), an oval basin represents a moderately active basin, an elongated basin represents an active tectonic environment, and a circular basin represents an inactive setting. Schumm (1956) provided the following equation, which is used to determine this parameter.

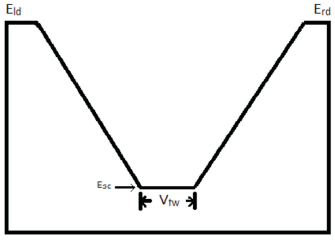

Fig. 6. Idealized diagram showing V_f.

$$E_b = 2\frac{\sqrt{A_b/\pi}}{l_b}$$

Where,E_b is the elongation ratio, A_b is the area of the basin, and l_b is the maximum length of the basin as measured for the relief ratio of the watershed. According to Chow (1964a), depending on climatic and geological types Basin elongation ratio (E_b), ranges from 0.6 for elongate and tectonically active basins to 1.0 for tectonically quiescent. Based on these standards, Chow (1964b) classified drainage basins as follows: circular (>0.9), oval (0.8-0.9), less elongate (0.7-0.8) and elongate (<0.7). Molin *et al*., (2004) notice that in active uplifting landscapes, youthful basins are relatively elongated. Bull and McFadden (1977) considered low values for basin elongation ratio as a proxy indicator of recent tectonic activity. Venuprasad *et al.* (2022) and Kamble *et al.* (2019)

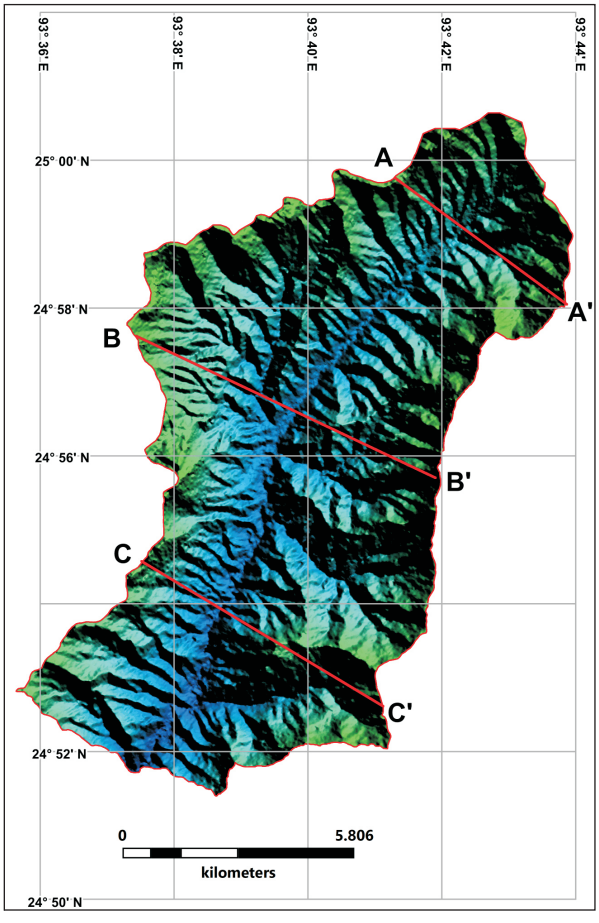

Fig.7a. Sections for V_f calculation.

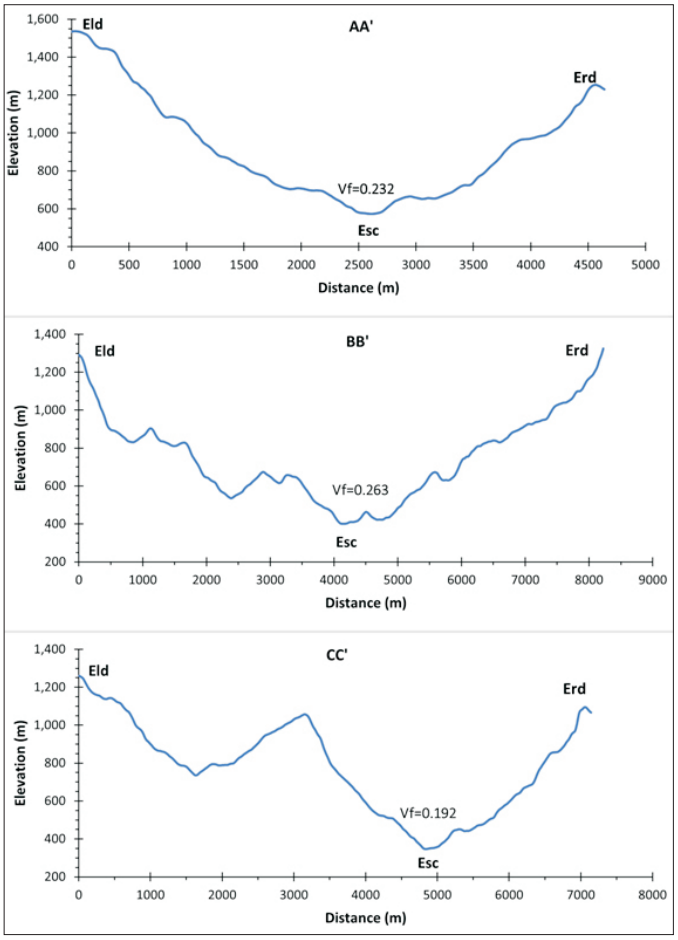

Fig.7b. Profiles for calculation of V_f.

suggest higher value of elongation ratio suggest comparatively flat terrain and lower value indicates a steep gradient with high relief. The calculated E_b value of Iring River Basin is 0.66 which is less than 0.7 (Table 2) indicating it as a tectonically active basin.

Hypsometric Curve and Integral

The hypsometric curve of a catchment, as outlined by Strahler (1952), illustrates the relative area below or above a specified altitude and serves as a gauge for the geomorphic maturity of a basin. This curve is a powerful tool for distinguishing between tectonically active and inactive regions, as noted by Keller and Pinter (1996). It not only reveals the erosional stage of the basin but also sheds light on the influence of tectonic activity, climate, and lithology (Moglen and Bras , 1995; Willgoose and Hancock, 1998; Huang and Niemann, 2006). The hypsometric integral (Hi), derived from the shape of the hypsometric curve, provides valuable insights into the terrain's elevation compared to the mean. High Hi values typically indicate elevated topography, such as upland surfaces carved by deeply incised streams, while intermediate and low values suggest extensive erosion and more evenly dissected drainage basins. Consequently, high values are associated with youthful or young landforms, whereas low values correspond to older formations (Strahler, 1952; Demoulin, 1998; Keller and Pinter, 2002). The calculation of the hypsometric integral, as described by Pike and Wilson (1971), follows a specific procedure.

$$H_i = \frac{H_{mean} - H_{min}}{H_{max} - H_{min}}$$

Where H_i is the hypsometric integral, H_{mean} is the mean elevation, and H_{min} and H_{max} are the lowest and highest elevations of the basin, respectively. $H_{min,}$ $H_{max,}$ H_{mean} and all required parameters for estimating the hypsometric integral are calculated using ArcGis's Raster calculator and Zonal statistics tools. Hypsometric curve for the basin is created by plotting relative area (a/A) against relative height (h/H), where "a" is the surface area within the basin above a given line of elevation. "A" is the total area of the basin. "h" is the elevation for which the value is to be calculated, and "H" is the highest elevation of the basin.

The calculated H_i value for Iring river basin is 0.50 % and its S-shaped hypsometric curve (Fig. 8) indicates early mature stage under the cycle of erosion, thereby tectonically active character of the watershed.

Drainage Basin Asymmetry (AF)

The asymmetry factor (AF) aids in assessing tectonic activity by analyzing the tilt of a river basin, as discussed by Keller and Pinter (1996). The movement of the trunk stream within a drainage basin is influenced by tectonic tilting, as highlighted by Morrish (2015). This perpendicular tilt, reflected in the asymmetry factor, serves as a key indicator of tectonic activity within a river basin, as noted by Cox (1994) and Tsodoulos *et al*. (2008). Drainage systems formed under active tectonic deformation exhibit distinct patterns and geometries.

The asymmetry factor was developed to detect tectonic tilting (Hare and Gardner, 1984) and is defined as follows:

$$AF = 100\,(A_r / A_t)$$

Where AF is the asymmetry factor, A_r is the area of drainage basin to the right side of trunk channel when facing downstream. AF should be equal to 50, for a main channel that formed and continues to flow in a stable setting. Whereas, AF greater or less than 50 would decide the tilt (Keller and Pinter 1996). Tilting of a watershed may be due to a fault as established in various river basins (Masurkar *et al.*, 2019; Manjare, 2015). The calculated value of AF is shown in Table 2 and its value of 47.72 % indicates the channel has shifted downstream right side of the Iring basin with an upliftment of eastern side which may be due to the Langka Fault (Fig. 9).

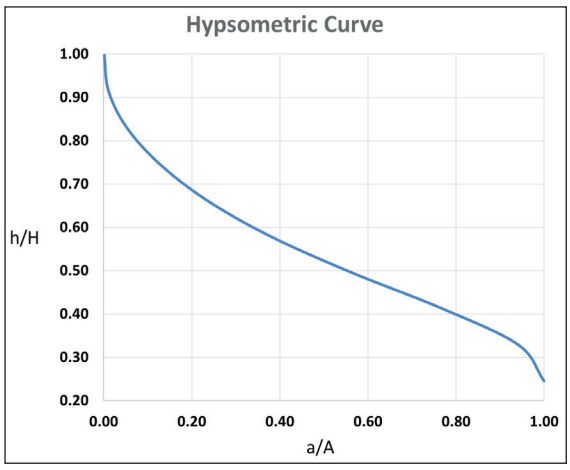

Fig.8. Hypsometric curve of Iring Watershed.

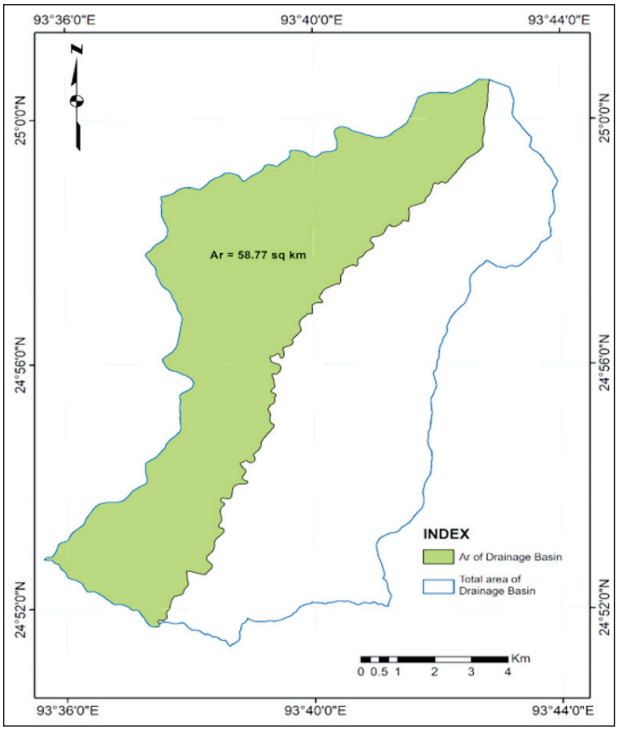

Fig.9. Diagram representing total area and right-side area of the Iring watershed when facing downstream.

Transverse Topography Symmetry Factor

The Transverse Topography Symmetry Factor provides insight into the asymmetry of a basin, aiding in the identification of the tilt direction and magnitude of a river in relation to active tectonics (Cox, 1994). An asymmetrical river basin is indicated by a value greater than zero (Keller and Pinter, 1996). This factor is computed using the equation provided below.

$$T = D_a / D_d$$

Where T is the transverse topographic symmetry factor, D_a is the distance from the midline of the drainage basin to the midline of active meander belt, and D_d is the distance from midline of the basin to the drainage divide (Fig. 10). According to Cox (1994), for perfectly symmetric basin T = 0, as the asymmetry increases, T approaches to the value of 1.

The traverse topography symmetry factor (T) for the Iring river basin has been calculated along the tributaries Iring. The calculated values for Iring are 0.282, 0.068, 0.155, 0.185, 0.298, 0.312, 0.163 and 0.098 for location a, b, c, d, e, f, g and h, respectively. The average value is 0.195, which is greater than 0 indicating asymmetric nature according to the Cox (1994).

Conclusions

After analyzing various geomorphic indices such as SL/K, valley floor width to valley height ratio, basin elongation ratio, hypsometric curve and its integral, drainage basin asymmetry, and transverse topography symmetry factor, it is evident that the study area exhibits signs of tectonic activity. The examination of the longitudinal profile yields valuable insights into the morphotectonic nature of the Iring watershed. Calculated parameters like the asymmetry factor (AF = 47.72%) and transverse topography symmetry factor (T = 0.195) indicate that the left side of the watershed is uplifted, causing the Iring river to shift towards the right side when viewed downstream. The hypsometric curve further supports the conclusion that the watershed ongoing tectonic activity. Additionally, the other parameters demonstrate a correlation between erosive power and tectonics. The study shows the dominance of tectonic forces over erosion evident across all studied parameters.

Table 2: Calculated geomorphic indices of Iring watershed

Sl. No.	Geomorphic indices	Value	Remarks
1	Basin Area (A)	118.67 km^2	Total basin area
3	H_{max}	1729 m	
4	H_{min}	281 m	
5	Hypsometric integral (H_i)	0.5	It shows youthful to mature basins
6	Basin elongation ratio (E_b)	0.66	Reflects elongate basin and tectonically active
7	Drainage basin asymmetry (A_F)	47.72 %	Tilted basin in nature
8	Transverse topography Symmetry (T)	0.195	
9	Valley floor width to valley height ratio (V_f)	0.192 to 0.263	
10	Basin perimeter	54.45 km	

Authors' Contributions

YSS: Conceptualization, Methodology, Investigation and Draft Manuscript. **YRS**: Investigation, Manuscript Reviewing and

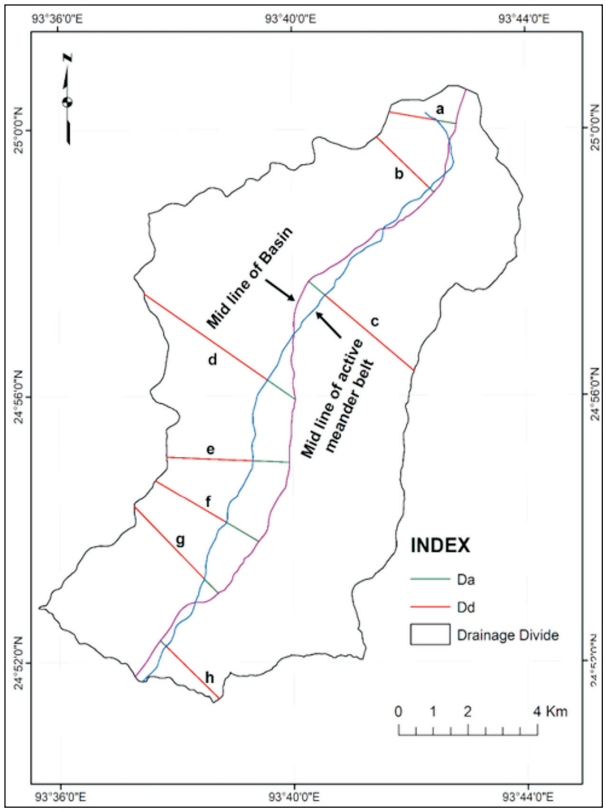

Fig.10. Transverse Topography symmetry of Iring watershed.

Editing. **MS**: Data analysis and GIS Software. **AK**: Supervision, Reviewing and Editing.

Conflict of Interest

The authors declared no conflict of interest.

Acknowledgements

The first author acknowledges the support extended by the Department of the Earth Sciences, and the GIS facilities provided by Seismological Observatory, Manipur University during the preparation of the manuscript.

References

Ahmad, S. and Bhat, M.I. (2012). Tectonic geomorphology of Rambiara basin, SW Kashmir Valley reveals emergent out-of-sequence active fault system. Him. Geol., v. 33(2), pp. 162-172.

Ahmad, S., Bhat, M.I., Madden, C. and Bali, B.S. (2013). Geomorphic analysis reveals active tectonic deformation on the eastern flank of the Pir Panjal Range, Kashmir Valley, India. Arabian Jour. Geosci., doi:10.1007/s12517-013-0900-y

Argyriou, A.V. and Teeuw, R.M. (2016). GIS multi-criteria decision analysis for assessment and mapping of neotectonic landscape deformation; a case study from Crete. Geomorphology, v. 253, pp. 262-274.

Azor, A., Keller, E.A. and Yeats, R.S. (2002). Geomorphic indicators of active fold growth; South Mountain-Oak Ridge Ventura basin, Southern California. Geol. Soc. Am. Bull., v. 114, pp. 745-753.

Bhattacharya, F., Rastogi, B.K. and Kothyari, G.C. (2013). Morphometric evidence of seismicity around Wagad and Gedi Faults, eastern Kachchh, Gujarat. Jour. Geol. Soc. India, v. 81, pp. 113-121.

Bull, W.B. and McFadden, L.D. (1977). Tectonic geomorphology north and south of the Garlock Fault, California. *In*: Arid Regions: Proc. Eighth Annu. Geomorph. Sym., State Univ. New York, Binghamton, pp. 115-138.

Burbank, D. and Anderson, R. (2001). Tectonic Geomorphology. Blackwell Science, Oxford. Strahler, A., 1952. Dynamic Basis of Geomorphology. Geol. Soc. Am. Bull., v. 63, pp. 923-938.

Chen, Y.C., Sung, Q. and Cheng, K.Y. (2003). Along-strike variations of morphotectonic features in the Western Foothills of Taiwan: tectonic implications based on stream gradient and hypsometric analysis. Geomorphology, v. 56(1), pp. 109-137.

Chow, V.T. (1964a). Handbook of applied hydrology: a compendium of water resources technology. McGraw Hill, New York, pp. 4-11.

Chow, V.T. (1964b). Handbook of applied hydrology: a compendium of water resources technology. McGraw Hill, New York, pp.7-10.

Cox, R.T. (1994). Analysis of drainage basin symmetry as a rapid technique to identify areas of possible Quaternary Tilt-block tectonics: an example from the Mississippi Embayment. Geol. Soc. Am. Bull., v. 106, pp. 571-581.

Demoulin, A. (1998). Testing the tectonic significance of some parameters of longitudinal river profiles: the case of the Ardenne (Belgium,NW Europe). Geomorphology, v. 24(2), pp. 189-208.

El Hamdouni, R., Irigaray, C., Fernandez, T., Chacón, J., Keller, E.A. (2007). Assessment of relative active tectonics, southwest border of SierraNevada (southern Spain). Geomorphology, v. 96, pp. 150–173.

Evans, P. (1932): Tertiary succession of Assam. Trans. Min. Geol. Inst., v. 27(23), pp. 155-260.

Evans, P. (1964) The tectonic framework of Assam. Jour. Geol. Soc. India, v. 5, pp. 80-96.

Geological Survey of India (1992). Geology and Structure of the areas around Tupul, Kharam, Houchong, Ponlen and Kabuikhul, Tamenglong District, Manipur. (For restricted circulation).

Hack, J.T. (1973). Stream-profile analysis and stream gradient index. US Geol. Surv. Jour. Res., v.1, pp.1421-1429.

Hare, P.H. and Gardner, T.W. (1985). Geomorphic indicators of vertical neotectonism along converging plate margins, Nicoya Peninsula, Costa Rica. In: Morisawa, M., Hack, J.T. (Eds.), Tectonic Geomorphology. Allen and Unwin, Boston, pp. 75-104.

Huang, X.J. and Niemann, J.D. (2006). Modelling the potential impacts of groundwater hydrology on long-term drainage basin evolution. Earth Surf. Process Landform, v. 31, pp. 1802-1823.

Kamble, P.B., Shinde, J.U., Herlekar, M.A., Gawali, P.B., Umrikar, B.N., Varade, A.M. and Aher, S. (2019). Morphometric Analysis of Ratnagiri Coast, Western Maharashtra, Using Remote Sensing and GIS Techniques. Jour. Geosci. Res., v. 4(2), pp. 185-195.

Keller, E.A. (1986) Investigation of active tectonics: use of surficial Earth processes. *In*: Wallace, R.E. (*Ed.*), Active Tectonics. Studies in Geoph. National Academy Press, Washington DC, pp.136-147.

Keller, E.A. and Pinter, N. (1996). Active tectonics: earthquakes uplift and landscapes. 2nd. Prentice Hall, New Jersey, 338p.

Keller, E.A. and Pinter, N. (2002). Active Tectonics: Earthquakes, Uplift, and Landscape, second ed. Englewood Cliffs, New Jersey, Prentice Hall, 362p.

Kirby, E., Whipple, K.X., Tang, W. and Chen, Z. (2003). Distribution of active rock uplift along the eastern margin of the Tibetan Plateau; inferences from bedrock channel longitudinal profiles. Jour. Geophy. Res., v.108(4), 24p.

Mallet, F.R. (1876). On the coal fields of Naga Hills bordering Lakhimpur and Sibsagar districts, Assam. Mem. Geol. Surv. India, v. 12(2). 286p.

Manjare, B.S. (2015). Morphotectonic Analysis of Upper Tapi River Sub-basin, Madhya Pradesh. Jour. Geosci. Res., v. 1(1), pp. 81-88.

Masurkar, S.P., Manjare, B.S. and Anusha, N. (2019). Morphotectonics of Wan River Sub-basin Using Remote Sensing and GIS Approach. Jour. Geosci. Res., v. 4(2), pp. 163-172.

Moglen, G.E. and Bras, R.L. (1995). The effect of spatial heterogeneities on geomorphic expression in a model of basin evolution. Water Resour. Res., v. 31, pp. 2613-2623.

Molin, P., Pazzaglia, F.J. and Dramis, F. (2004). Geomorphic expression of active tectonics in a rapidly-deforming forearc, Sila Massif, Calabria, Southern Italy. Am. Jour. Sci., v. 304, pp. 559-589.

Morrish, S.C. (2015). Characterization and Digital Morphotectonic Analysis of Drainage Basins in a Deforming Forearc, Nicoya Peninsula, Thesis: California State Polytechnic University, Pomona.

Mukteshwar, N.M. (2019). Active tectonic deformation of the Shillong plateau, India: Inferences from river profiles and stream-gradients. Jour. Asian Earth Sci., v. 181, pp. 1-23.

Pérez-Peña, J.V., Azañón, J.M., Azor, A., Delgado, J. and González-Lodeiro, F. (2009). Spatial analysis of stream power using GIS: SLk anomaly maps. Earth Surf. Proc. Land., v. 34, pp. 16-25. https://doi.org/10.1002/esp.1684.

Pérez-Peña, J.V., Azor, A., Azañón, J.M. and Keller, E.A. (2010). Active tectonics in the Sierra Nevada (Betic Cordillera, SE Spain): insights from geomorphic indexes and drainage pattern analysis. Geomorphology, v.119, pp. 74-87. https://doi.org/10.1016/j.geomorph. 2010.02.020.

Pike, R.J. and Wilson, S.E. (1971). Elevation relief ratio, hypsometric integral and geomorphic area-altitude analysis. Geol. Soc. Am. Bull., v. 62, pp. 1079-1084.

Rockwell, T.K., Keller, E.A. and Johnson, D.L. (1985). Tectonic geomorphology of alluvial fan sand mountain front near Ventura, California. *In*: Morisawa, M., Hack, J.T. (*Eds.*), Tectonic Geomorphology –Proceedings of the 15th Annual Binghampton Geomorph. Symp. Sep. 1984. Allen and Unwin, pp. 183-208.

Schumm, S.A. (1956). Evolution of Drainage Systems and Slopes in Badlands at Perth Amboy, New Jersey. Geol. Soc. Am. Bull., v. 67, pp. 597-646.

Snow, R.S. and Slingerland, R.L. (1987). Mathematical modelling of graded river profiles. Jour. Geol., v. 95, pp. 15-33.

Soibam, I. (1998). Structural and Techtonic analysis of Manipur with special reference to evolution of the Imphal Valley; Unpublished Ph.D. Thesis, Manipur University.

Sreedevi, P.D., Subrahmanyam, K. and Shakeel, A. (2004). The significance of morphometric analysis for obtaining groundwater potential zones in a structurally controlled terrain. Env. Geol., v. 47(3), pp. 412-420.

Strahler, A. (1952). Dynamic Basis of Geomorphology. Geol. Soc. Am. Bull., v. 63, pp. 923-938.

Tapponnier, P. and Molnar, P. (1976). Slip line field theory and large-scale continental tectonics. Nature, v. 264 (5584), pp. 319-324.

Tsodoulos, I.M., Koukouvelas, I.K. and Pavlides, S. (2008). Tectonic geomorphology of the easternmost extension of the Gulf of Corinth (Beotia, Central Greece). Tectonophysics, v. 453, pp. 211-232.

Venuprasad, A., Nagaraju, D., Manjunath, K. and Pramoda, G. (2022). Morphometric Interpretation for Sub-Basin Management Planning and Practices in Hassan District, Karnataka India Using GID and Remote Sensing, Jour. Geosci. Res., v. 7(2), pp. 227-234.

Wells, S.G., Bullard, T.F., Menges, T.M., Drake, P.G., Karas, P.A., Kelson, K.I., Ritter, J.B. and Wesling, J.R. (1988). Regional variations in tectonic geomorphology along segmented convergent plate boundary, Pacific Coast of Costa Rica. Geomorphology, v. 1, pp. 239-265.

Willgoose, G. and Hancock, G. (1998). Revisiting the hypsometric curve as an indicator of form and process in transport-limited catchment. Earth Surf. Process Landform., v. 23, pp. 611-623.